

Numerical Evaluation of the Performance Efficiency of Small-Caliber Colonoscopes in Reducing Patient Pain during a Colonoscopy: Influence of Gender

Xuehuan He¹, Jing Bai¹, and Debao Zhou^{1,2}

¹University of Minnesota Duluth, Duluth, MN, USA, 55812

²Tianjin Polytechnic University, Tianjin, China, 300387

Email: {hexxx977, jingbai, dzhou}@d.umn.edu

Abstract—This paper presents the development of an insertion simulation of colonoscopes with different diameters inside colon models using ANSYS LS-DYNA. The purpose is to provide insight on the performance efficiency of small-caliber (SC) colonoscopes in reducing patient pain during a colonoscopy considering the effect of gender. In developing such a simulation, the structural differences between the female and male human colons were firstly analyzed and further used as the basis of establishing colon models. The colonic tissue was comprised of a three-parameter Mooney Rivlin model whose parameters were obtained through an optimization procedure with the use of ANSYS and Optislang programs. Colon deformation induced by colonoscopes during the insertion simulation were investigated to provide prediction of patient pain. The simulation results show that colonoscopes with smaller diameters may be helpful in reducing patient pain for females while having no or less advantage for males.

Index Terms—ANSYS LS-DYNA, Small-Caliber (SC) colonoscope, patient pain, gender, colon deformation

I. INTRODUCTION

One of the main complications in completing a colonoscopy is that the colonoscope causes patient pain during the insertion procedure [1]. Recently, Small-Caliber (SC) colonoscopes, including Pediatric Colonoscope (PDC) and Ultrathin Colonoscope (UTC), have been designed to facilitate difficult colonoscopy [2]-[5]. To evaluate the efficacy of the SC colonoscopes in reducing patient pain, a Randomized Controlled Trial (RCT) conducted in [6] compared the performance efficiency of a newly developed SC colonoscope with that of a Standard Colonoscope (SDC), in female and male patients. The results showed that the maximum and overall pain during colonoscopy were significantly lower in the small-caliber group than in the standard group in women, whereas no significant differences were seen in men. However, the SC colonoscope developed in this study was also equipped with many other new technical

features, including a high force transmission shaft, a variable stiffness shaft and a passive bending. These have been proved to be helpful in reducing patient pain through previous researches [7], [8]. As a result, the influence of the diameter of the scope shaft itself on the patient pain is still unclear. Meantime, in RCT, endoscopists were not blinded to the colonoscope, thus their skills may largely affect the result and limited the generalizability of the finding.

To explore the influence of gender of patients on the efficacy of SC colonoscopes in reducing patient pain, a numerical model could provide such insight is developed in our work. An explicit solver ANSYS-LSDYNA was selected to simulate the insertion process of colonoscopes in colon models. Patient pain is predicted through comparing the colon deformation during the insertion simulation. Such a model could also overcome the limitation of RCT, i.e. the skills of endoscopists.

II. MODEL SETUP

A. Colon Model

Previous studies investigated the colonic length and mobility for female and male colons [9], [10]. The results showed that although there were no significant differences in rectum plus sigmoid, descending, or ascending plus cecum segmental lengths, women had longer transverse colons. At the same time, there were no differences in mobility of the descending colon and transverse colon between the sexes, but the transverse colon reached the true pelvis more often in women than in men. As a result, the segments of colon: transverse colon, hepatic flexure and ascending colon were selected to develop colon models while representing the gender induced structural differences for the human colon.

Based on the studies about colon anatomy in [11], the idealized colon model was assumed as a thin-walled tube with uniform thickness and internal diameter in this work. Fig. 1 illustrates the spline used for developing the colon model in our work. A 10cm straight line was selected to represent the centre line of ascending colon while an arc

with radius (R) equals to 5cm for hepatic flexure [12] [13]. The transverse colon has a typical triangular configuration and is enveloped by the transverse mesocolon peritoneum. The degree of droop of the transverse colon towards the pelvis accounts for the variable bowel length and affects the acuteness of the hepatic flexure bend [14]. It is reported that for persons of normal body mass index, abdominal diameter should be under 25 cm [15]. At the same time, the mean abdominal wall thickness is 22 mm [16]. Therefore, the straight distance between splenic and hepatic flexure was selected as 20cm. An angle β was equipped with 0° , 30° and 45° to account for the change of curvature and length of the transvers colon as shown in Fig. 1.

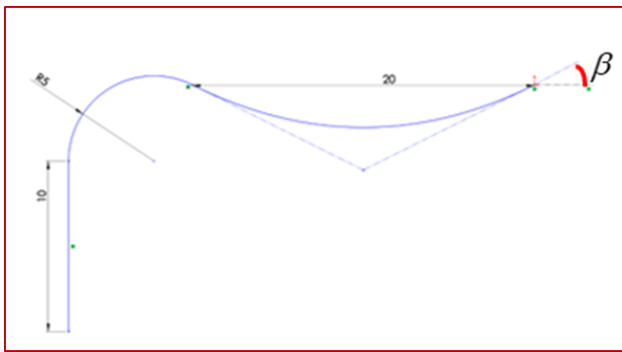


Figure 1. Spline used for colon model.

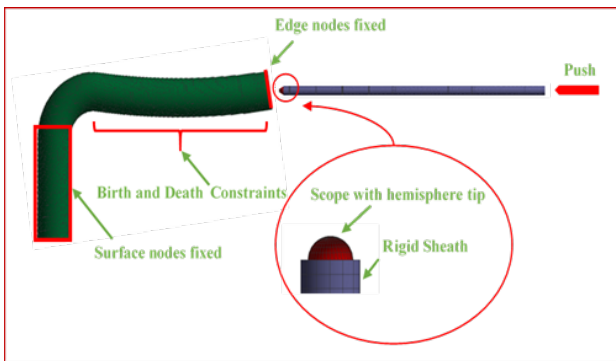


Figure 2. Mesh and boundary conditions for the colonoscopy insertion simulation.

A constraint model attempted in [17] was used as a basis for this simulation. To investigate the deformation of transverse colon due to the intubation of colonoscopes, in this study, edge nodes of the free end of transverse colon, surface nodes of ascending colon and hepatic flexure were fixed as shown in Fig. 2. Colon was meshed with Discrete Kirchhoff Triangular (DKT) triangular shell elements.

The mechanical stretch of colon induced by the colonoscope during the insertion process is mainly along its longitudinal direction, thus we chose to characterize the longitudinal behaviour of the colonic wall using an isotropic and incompressible three-parameter Mooney Rivlin hyperelastic model as shown in (1).

$$W = C_{10}(I_1 - 3) + C_{01}(I_2 - 3) + C_{11}(I_1 - 3)(I_2 - 3) \quad (1)$$

The optimized material parameters for C_{10} , C_{01} and C_{11} were identified through an optimization procedure as shown in section 3. A density of $\rho=1040\text{kg/m}^3$ was applied for the colonic tissue [18].

B. Colonoscope Model

The colonoscope was modelled as a cylinder with a hemisphere tip and meshed with 8 nodes brick element. The colonoscope was pushed into colon models by prescribing a ramp motion function with a constant velocity to the set of nodes located at their lower end as shown in Fig. 2. To prevent the buckling of the colonoscope before entering the colon model, a rigid sheath was introduced in our model as shown in Fig. 2. Three different diameters of colonoscopes, including a 13.3 mm SDC, a 11.1mm PDC and a 9.2 mm UTC with length of 50cm for insertion simulation inside the colon model were studied.

As for the properties of the colonoscope, the complex and sensitive internal components of colonoscope make it difficult to obtain the mechanical properties (Young's modulus) from stress-strain relationship like colon through tensile test. Therefore, the Young's modulus of colonoscope used for simulation in our work was extracted from the flexural rigidity (EI) through 3-point bending test Conducted by [19]. As a result, a linear elastic material model was applied for the colonoscope model with a Young's Modulus of $E = 16\text{MPa}$, a density of $\rho = 2944 \text{kg/m}^3$ [20], and a Poisson's ratio of $\nu = 0.3$.

C. Input Motion Profile

It is known that an experienced endoscopist always straighten the sigmoid and transverse colon by torquing or pulling scope before pushing it to pass through the hepatic flexure to reduce the possibilities of loop formation [17]. Therefore, there exists the dynamic relaxation of the colonoscope between the action of straightening transverse colon and reinsertion into hepatic flexure. To compare the colon deformation induced by the buckling shaft of the colonoscope when it negotiates the hepatic flexures. In our work, birth and death constraints were used to control the lateral movement of transverse colon and the motion of scope to realize such process. Such a birth and death constraint could ensure the same straightening process and thus eliminating the influence of the disturbing factor, i.e., endoscopists' skills. The lateral movement of the transverse colon was set to be constrained from 0s to 0.6s and released after 0.6s while the input motion profile of the colonoscope is shown in Fig. 3.



Figure 3. Input motion profile of the colonoscope.

In this explicit simulation, to avoid the collapse of the elements under high frequent collision, the loading rate was limited to be less than 1% of the wave speed of the colonoscope [21]. At the same time, the simulations are

slightly accelerated by increasing the insertion rate of the colonoscope to achieve reasonable calculation times. As a result, the insertion velocity of the colonoscope is selected as 60cm/s in our work.

To ensure the quasi-static properties of the interaction between colon and colonoscope, a numerical contact damping was introduced in the model to dissipate vibration due to high push loading rate of the colonoscope. The numerical contact damping coefficient was adjusted to make the time increment for the explicit simulation up to $7e-6s$. Meanwhile, for both colon and colonoscope, we checked that the ratio of kinetic energy to internal energy remain lower than 10% for most of time during all simulations as can be attested by the energies plotted in Fig. 4 and Fig. 5.

III. TISSUE PARAMETERS OPTIMIZATION

In our work, the parameters C_{10} , C_{01} and C_{11} were identified through an optimization procedure with the use of ANSYS and Optislang programs. Numerical and experimental approaches were performed to realize such an optimization procedure.

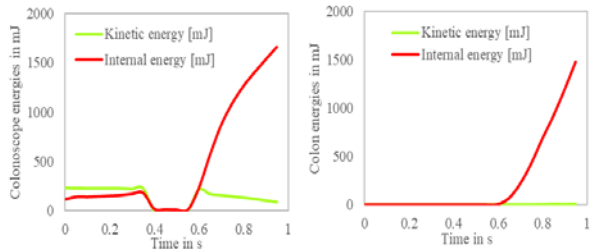


Figure 4. Average kinetic energy and internal energy evolution for colon and SDC.

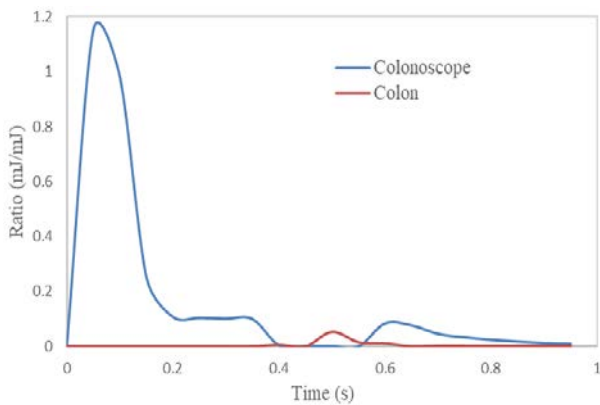


Figure 5. Ratio of kinetic energy to internal energy for colonoscope and colon.

A. Experimental Details

A uniaxial tension test of porcine colon at a quasi-static loading rate of 1cm/min was conducted as shown in Fig. 6 to find the raw load-displacement curve. 8 specimens from different parts of the porcine colon tissue were prepared. The mean force-displacement curve was shown in Fig. 7, which shows highly nonlinear relationship.



Figure 6. Experimental set-up.

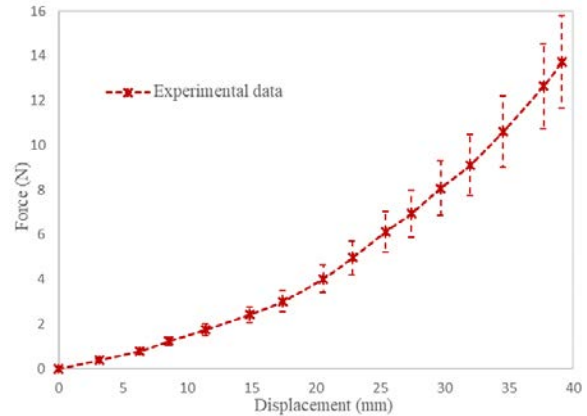


Figure 7. Mean experimental force-displacement response of porcine colon.

B. Computational Model

As the colon is almost an incompressible hyperelastic material, 4-node shell elements with the capability of modelling this material were used to construct a 3D finite element (FE) model of the colon specimen as shown in Fig. 8. When displacement load was applied onto the right surface, the total node reaction force F_{simu}^i in the left surface can be easily extracted through the signal processing after the FE program was executed. Based on the optimized results, the constitutive material parameters of the colon were input into the FE program.

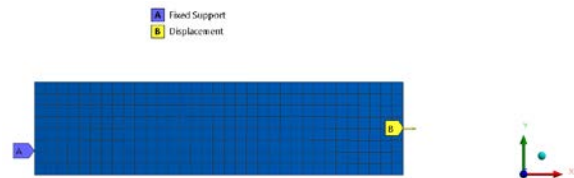


Figure 8. FE model of the Colon specimen.

C. Optimization Objective Function

Generally, the initial elastic modulus (E) for incompressible materials under infinitesimal strain conditions is given as (2).

$$E = 6(C_{10} + C_{01}) \quad (2)$$

The initial estimates of hyperelastic coefficients, C_{10} and C_{01} , were determined by setting them equals to each other. From the experiment result, the mean value of young's modulus for porcine colon tissue under strain

(10%) is 0.36Mpa and 2.5Mpa under the strain before the fracture of the specimen (60%). therefore, the initial guess for three parameters was given at

$$C_{10}=C_{01}=0.03Mpa; C_{11}=1.25Mpa$$

The optimization objective function is written in (3).

$$\text{Min} (e_j = \sqrt{\sum_{i=1}^k (F_i^{EXP} - F_i^{SIMU})^2}) \quad (3)$$

$$\text{s.t } C_{10}, C_{01} \in [0, 0.06Mpa], C_{11} \in [0, 2.5Mpa]$$

where k denotes the number of data samples, F_i^{EXP} is the experimental value of tensile force for the ith sample, and F_i^{SIMU} is the simulated data obtained from the ANSYS for the corresponding step, e_j is the discrepancy between the simulated and the experimental data.

D. Optimization Procedures and Results

The optimization flow chart proposed by [22] inside Optislang was used in this work. It took 38 iterations to find the best optimized result in our work. Fig. 9 showed the evolution of objective difference during the 38 iterations. The final optimized parameters are 652.01Pa, 42.8kPa, and 219.1kPa for C_{10} , C_{01} and C_{11} with $e_j=0.0845$. The optimized result was plotted as a solid line as shown in Fig. 10. It is noticed that there is good agreement between the simulated and experimental hyperelastic behaviour of the colon as represented by their force–displacement relations. Thus, it verified that the proposed optimization scheme for the parameters of Mooney–Rivlin model was reliable.

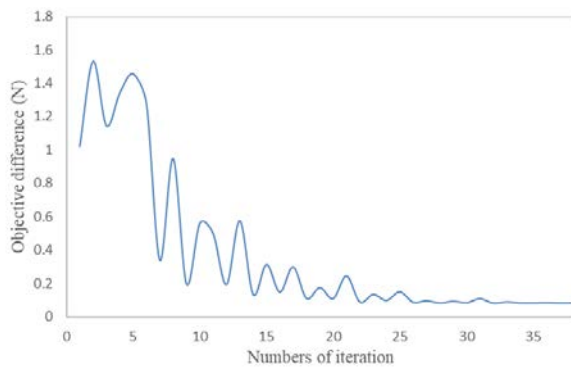


Figure 9. Evolution of objective difference along with the iteration.

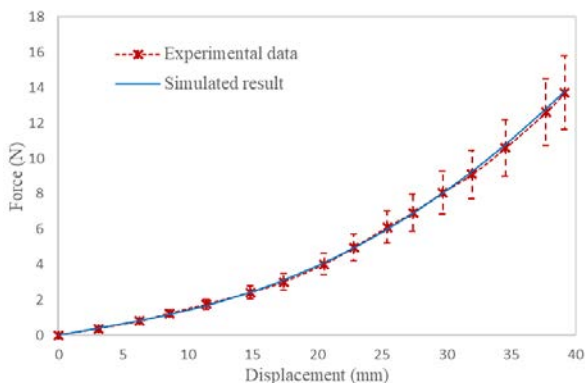


Figure 10. Final optimized design.

IV. RESULTS

In comparison to men, women tend to have a longer and deeper transverse colon. Therefore, in our study, an angle β as shown in Fig. 1 was introduced to represent the change of the length and curvature of the transverse colon. The insertion simulation for UTC, PDC and SDC in the colon model with $\beta=0^\circ, 30^\circ$ and 45° were simulated.

The final transverse colon deformation is shown in Fig. 11 while Table I summarized differences of final transverse colon deformation induced by SC colonoscopes with respect to that induced by SDC. It is noticed that: compared with the final transverse colon deformation induced by SDC, for $\beta=0^\circ$, UTC and PDC causes 0.37cm and 1.3cm more final transverse colon deformation than that caused by SDC. For $\beta=30^\circ$, UTC reduces 1.67 cm final transverse colon deformation while PDC shows slightly more final transverse colon deformation (0.12cm). For $\beta=45^\circ$, the reduction of final transverse colon deformation is 4.85 cm for UTC and 1.08 cm for PDC, respectively.

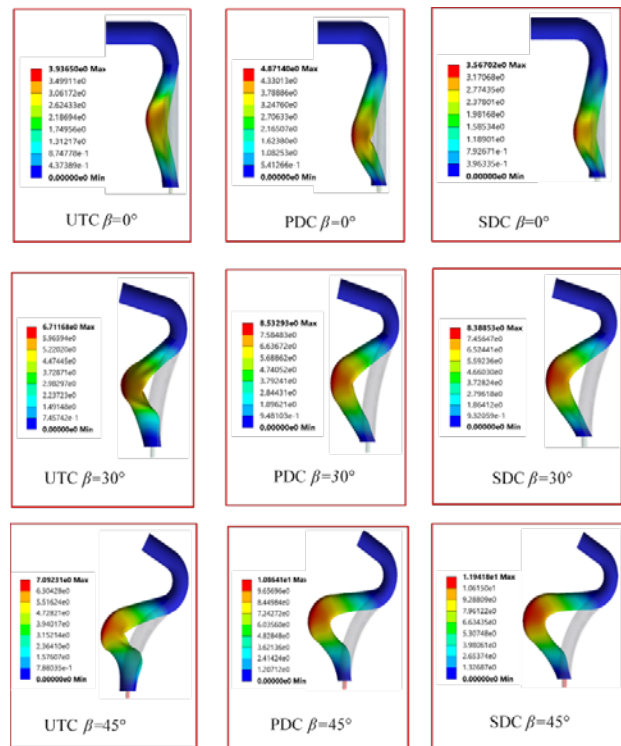


Figure 11. Final transverse colon deformation (cm).

TABLE I. DIFFERENCES OF FINAL TRANSVERSE COLON DEFORMATION INDUCED BY SC COLONOSCOPES WITH RESPECT TO THAT INDUCED BY SDC

Angle β	Difference with respect to SDC (cm)	
	UTC	PDC
0 deg	0.37	1.30
30 deg	-1.67	0.12
45 deg	-4.85	-1.08

Fig. 12, Fig. 13 and Fig. 14 demonstrates the plot for transverse colon deformation during the whole insertion simulation in colon models with $\beta=0^\circ, 30^\circ$ and 45° ,

respectively. For $\beta=0^\circ$, SC colonoscopes (UTC and PDC) cause slightly more colon deformation during whole insertion simulation. For $\beta=30^\circ$, PDC and SDC show almost the same colon deformation and are larger than that of the UTC. For $\beta=45^\circ$, SDC shows much more colon deformation than SC colonoscopes. Meanwhile, it can be observed that the difference of transverse colon deformation induced between SC colonoscopes and SDC show positive correlations with angle β .

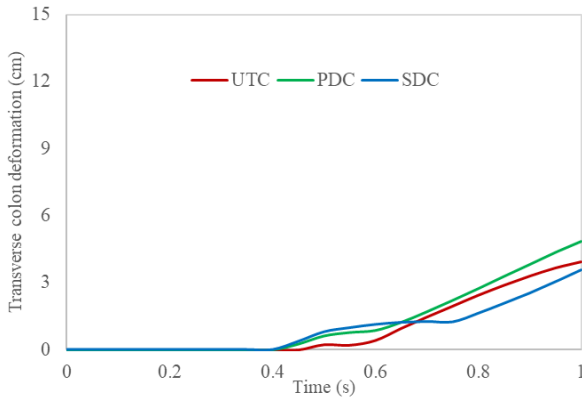


Figure 12. Transverse colon deformation ($\beta=0^\circ$).

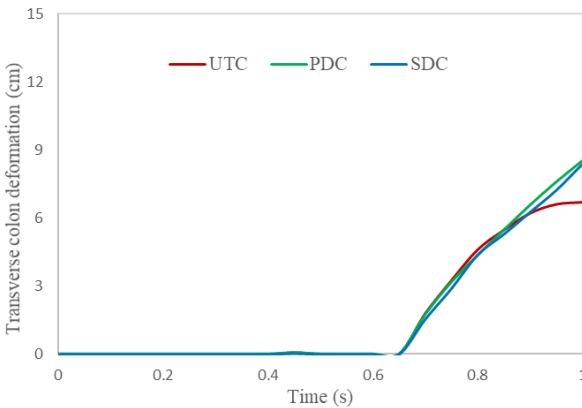


Figure 13. Transverse colon deformation ($\beta=30^\circ$).

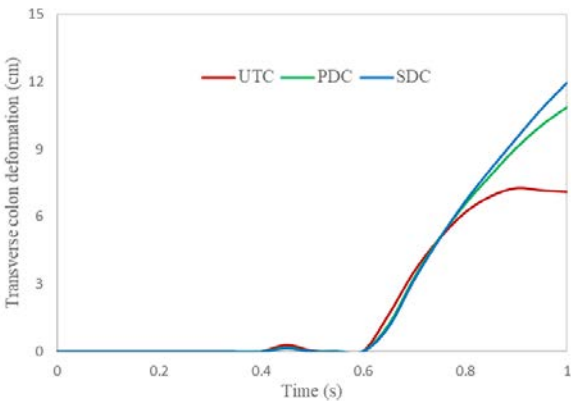


Figure 14. Transverse colon deformation ($\beta=45^\circ$).

The simulation results could be used to further predict the influence of gender of patients on performance efficiency of SC colonoscopes in reducing patient pain, i.e., SC colonoscopes (UTC and PDC) have no advantage

in reducing patient pain for men (colon model with small β) while they are more helpful in reducing discomfort for female patients (colon model with larger β).

V. DISCUSSIONS

There exist many limitations in our work, and further work remains to improve the simulation: (1) the colon model as well as boundary conditions were simplified in our work, which is not realistic for a complicate human colon structure, and thus potential errors in estimating the colon deformation may exist. Further work could be done in precisely reconstructing the geometry. Tools such as CT scan could be used for non-invasive detection and reconstruction. (2) We did not consider the anisotropic properties of colon tissue. Since the mechanical stretch of the colonic wall induced by a colonoscope is mainly along longitudinal direction, an isotropic, incompressible hyperelastic model was selected to model the tensile properties of colon tissue in our work. An anisotropic fiber-reinforced hyperelastic model would have led to more accurate characterizations of colonic tissue properties and could be applied in our future work. (3) we did not consider the influence of gender, on the material properties of the human colon. To include such influence in our model may lead to more accurate simulation results. Therefore, studying the differences of the material properties of the human colon with respect gender will be one of my future work. (4) The validation process by designing corresponding experiment was lacked in our work. However, no research has been found on the resultant displacement of the colon caused by the intubation of scope. That the simulation results prove to be realistic remains to be determined due to the lack of good test data.

VI. CONCLUSIONS

In this paper, a simulation of the insertion of colonoscopes with different diameters (UTC, PDC and SDC) inside colon models was successfully developed with an explicit FE solver, while the effects of the gender of patients were investigated. Instead of a whole human bowel model, three segments of the human colon which could represent the anatomical differences with respect to gender were modelled in our work. Patient pain induced by colonoscopes was predicted by comparing the colon deformation. As a result, the following results could be achieved based on our simulation, i.e., compared with the SDC, a SC colonoscope can help decrease patient pain for females while showing less or no advantage for males.

In sum, the simulation results in our work provide insight on how the gender of patients affect the efficacy of smaller-diameter colonoscopes in reducing patient pain during a colonoscopy. It may further provide a scientific guideline for the selection of a patient-specified colonoscope.

ACKNOWLEDGMENT

The authors appreciate LSTC for making LS-DYNA readily available for this research.

REFERENCES

[1] R. Mitchell, K. McCallion, K. Gardiner, R. Watson, and J. Collins, "Successful colonoscopy; completion rates and reasons for incompleteness," *The Ulster Medical Journal*, vol. 71, no. 1, pp. 34-37, 2002.

[2] D. K. Rex, "Achieving cecal intubation in the very difficult colon," *Gastrointestinal Endoscopy*, vol. 67, no. 6, pp. 938-944, 2008.

[3] R. A. Kozarek, V. A. Botoman, and D. J. Patterson, "Prospective evaluation of a small caliber upper endoscope for colonoscopy after unsuccessful standard examination," *Gastrointestinal Endoscopy*, vol. 35, no. 4, pp. 333-335, 1989.

[4] C. H. Park, W. S. Lee, Y. E. Joo, et al., "Sedation-free colonoscopy using an upper endoscope is tolerable and effective in patients with low body mass index: A prospective randomized study," *American Journal of Gastroenterology*, vol. 101, no. 11, pp. 2504-2510, 2006.

[5] T. Saifuddin, M. Trivedi, P. D. King, R. Madsen, and J. B. Marshall, "Usefulness of a pediatric colonoscope for colonoscopy in adults," *Gastrointestinal Endoscopy*, vol. 51, no. 3, pp. 314-317, 2000.

[6] K. Sato, S. Ito, F. Shigiyama, T. Kitagawa, K. Hirahata, Tominaga K, and I. Maetani, "A prospective randomized study on the benefits of a new small-caliber colonoscope," *Endoscopy*, vol. 44, no. 8, pp. 746-753, 2012.

[7] R. Rajagopalan, P. Deodurg, and Srikanth, "Overview of randomized controlled trials," *Asian Journal of Pharmaceutical and Clinical Research*, vol. 6, no. 3, pp. 32-38, 2013.

[8] A. Pasternak, M. Szura, R. Solecki, M. Matyja, A. Szczepanik, and A. Matyja, "Impact of responsive insertion technology (RIT) on reducing discomfort during colonoscopy: Randomized clinical trial," *Surgical Endoscopy*, vol. 31, no. 5, pp. 2247-2254, 2017.

[9] B. P. Saunders, M. Fukumoto, S. Halligan, C. Jobling, M. E. Moussa, C. I. Bartram, and C. B. Williams, "Why is colonoscopy more difficult in women?" *Gastrointestinal Endoscopy*, vol. 43, no. 2, pp. 124-126, 1996.

[10] R. Rowland, S. Bell, G. Dogramadzi, and D. Allen, "Colonoscopy aided by magnetic 3D imaging: Is the technique sufficiently sensitive to detect differences between men and women?" *Medical & Biological Engineering & Computing*, vol. 37, no. 6, pp. 673-679, 1999.

[11] M. L. Whitmer, "Clinical anatomy of the large intestine," *Centers for Osteopathic Research & Education*, 2007.

[12] C. R. Welch and J. D. Reid, "Looping formation during colonoscopy – a simulation," in *Proc. 14th International LS-Dyna Users Conference*, 2016.

[13] Blausen.com staff, "Blausen gallery 2014," *Wikiversity Journal of Medicine*, vol. 1, no. 2, 2014.

[14] V. Jayasekaran, et al., "Normal adult colonic anatomy in colonoscopy," *Video Journal and Encyclopedia of GI Endoscopy*, vol. 1, no. 2, pp. 390-392, 2013.

[15] C. Ribarren, J. A. Darbinian, J. C. Lo, B. H. Fireman, and A. S. Go, "Value of the sagittal abdominal diameter in coronary heart disease risk assessment: Cohort study in a large, multiethnic population," *American Journal of Epidemiology*, vol. 164, no. 12, pp. 1150-1159, 2006.

[16] D. Balaguru, U. Bhalala, M. Haghighi, and K. Norton, "Computed tomography scan measurement of abdominal wall thickness for application of near-infrared spectroscopy probes to monitor regional oxygen saturation index of gastrointestinal and renal circulations in children," *Pediatric Critical Care Medicine*, vol. 12, no. 3, pp. e145-e148, 2011.

[17] A. Loeve, P. Fockens, and A. Breedveld, "Mechanical analysis of insertion problems and pain during colonoscopy: Why highly skill-dependent colonoscopy routines are necessary in the first

place ... and how they may be avoided," *Canadian Journal of Gastroenterology*, vol. 27, no. 5, pp. 293-302, 2011.

[18] ICRU, Photon, Electron, Proton and Neutron Interaction Data for Body Tissues: ICRU Report 46. International Commission on Radiation Units and Measurements, Bethesda: ICRU, 1992.

[19] W. B. Cheng, et al., "Analysis of and mathematical model insight into loop formation in colonoscopy," *Proceedings of the Institution of Mechanical Engineers, Part H: Journal of Engineering in Medicine*, vol. 226, no. 11, pp. 858-867, 2012.

[20] A. Eickhoff, J. Van Dam, R. Jakobs, V. Kudis, D. Hartmann, and J. F. Riemann, "Computer-assisted colonoscopy (the NeoGuide system): Results of the first human clinical trial," *Am J Gastroenterol.*, vol. 102, no. 2, pp. 261-266, 2006.

[21] Livermore Software Technology Corporation, *LS-DYNA, 2013 Theoretical Manual (R 7.0)*, 2013.

[22] S. Kunath, et al., "Effective Parameter Identification to Validate Numerical Simulation Models," in *Proc. NAFEMS World Congress*, 2015.



Xuehuan He received the B.S. degree with distinguished thesis from the school of Mechanical Engineering, Chang'an University, China in 2015. She got her M.S. degree in Mechanical Engineering at University of Minnesota Duluth (UMD) in 2018. She is pursuing Ph.D. degree in the University of Iowa. Her research interests include Biomechanics and Machine Learning.



Jing Bai is a professor and the Director of Graduate Studies in the Department of Electrical Engineering at UMD. She received her PhD degree and MSc degree in electrical and computer engineering at Georgia Institute of Technology in 2007 and 2003, respectively. She also earned the MEng degree in Nanyang Technological University, Singapore, in 1999 and the BEng degree in Tsinghua University, China, in 1996, both in mechanical engineering. Her current research activities focus on nanoscale pielectronics and photovoltaics, nonlinear optics, plasmonics, biomedical engineering, and micro-electro-mechanical system (MEMS). She is a member of the Institute of Electrical and Electronics Engineers (IEEE), IEEE Women in Engineering (WIE), the Optical Society of America (OSA), and the American Physics Society (APS).



Debao Zhou is a professor and the Director of Graduate Studies in the Department of Mechanical and Industrial Engineering at UMD. From 2005 to 2008, he was with Georgia Tech Research Institute as a Postdoctoral fellow. He received his Ph.D. degree in Mechanical and Production Engineering in Nanyang Technological University, Singapore in 2004. He also earned his Master of Engineering degree and Bachelor of Engineering degree from Tsinghua University, P. R. China both in Mechanical Engineering. His active research interests include distributed force sensor design, modeling of bio-material cutting, design of next generation endoscope, tracking system development using thermal imaging method, and system dynamics and control.